









Overexpression of NDR1 leads to pathogen resistance at elevated temperatures

Saroopa P. Samaradivakara^{1,2} , Huan Chen^{3,4} , Yi-Ju Lu^{1,5} , Pai Li^{1,6} , Yongsig Kim¹ , Kenichi Tsuda^{7,8,9} , Akira Mine¹⁰  and Brad Day^{1,2,3,4} 

¹Department of Plant, Soil and Microbial Sciences, Michigan State University, East Lansing, MI 48824, USA; ²Plant Resilience Institute, Michigan State University, East Lansing, MI 48824, USA; ³Graduate Program in Genetics and Genome Sciences, Michigan State University, East Lansing, MI 48824, USA; ⁴Graduate Program in Molecular Plant Sciences, Michigan State University, East Lansing, MI 48824, USA; ⁵Institute of Biochemistry, National Chung Hsing University, Taichung 402, Taiwan; ⁶Department of Plant Biology, Michigan State University, East Lansing, MI 48824, USA; ⁷State Key Laboratory of Agricultural Microbiology, Hubei Hongshan Laboratory, Hubei Key Lab of Plant Pathology, College of Plant Science and Technology, Huazhong Agricultural University, Wuhan 430070, China; ⁸Shenzhen Institute of Nutrition and Health, Huazhong Agricultural University, Wuhan 430070, China; ⁹Shenzhen Branch, Guangdong Laboratory of Lingnan Modern Agriculture, Genome Analysis Laboratory of the Ministry of Agriculture and Rural Affairs, Agricultural Genomics Institute at Shenzhen, Chinese Academy of Agricultural Sciences, Shenzhen 518120, China; ¹⁰Laboratory of Plant Pathology, Graduate School of Agriculture, Kyoto University, Kyoto 606-8502, Japan

Summary

- Abiotic and biotic environments influence a myriad of plant-related processes, including growth, development, and the establishment and maintenance of interaction(s) with microbes. In the case of the latter, elevated temperature has been shown to be a key factor that underpins host resistance and pathogen virulence.
- In this study, we elucidate a role for *Arabidopsis* NON-RACE-SPECIFIC DISEASE RESISTANCE1 (NDR1) by exploiting effector-triggered immunity to define the regulation of plant host immunity in response to both pathogen infection and elevated temperature.
- We generated time-series RNA sequencing data of WT Col-0, an *NDR1* overexpression line, and *ndr1* and *ics1-2* mutant plants under elevated temperature. Not surprisingly, the *NDR1*-overexpression line showed genotype-specific gene expression changes related to defense response and immune system function.
- The results described herein support a role for NDR1 in maintaining cell signaling during simultaneous exposure to elevated temperature and avirulent pathogen stressors.

Author for correspondence:
Brad Day
Email: bday@msu.edu

Received: 6 January 2022
Accepted: 19 April 2022

New Phytologist (2022) **235**: 1146–1162
doi: 10.1111/nph.18190

Key words: *Arabidopsis*, effector-triggered immunity (ETI), heat stress, NON-RACE-SPECIFIC DISEASE RESISTANCE-1 (NDR1), *Pst*-AvrRpt2, salicylic acid.

Introduction

Plant response to abiotic and biotic stress requires the coordinated activity of numerous cellular processes, the vast majority of which share overlapping functions in basic physiological programs, including growth, development, and reproduction (Nejat & Mantri, 2017; Saijo & Loo, 2020). In recent years, the impact of elevated temperature on plant growth and defense has received increasing attention, due in part to ongoing changes in global climate and environmental stress (Havko *et al.*, 2020; Zhao *et al.*, 2020; Zhang *et al.*, 2022). However, the precise mechanisms that govern immunity at elevated temperature remain undefined.

Plant growth, development, and immune signaling processes are each influenced by fluctuations in temperature and environment (Zhu *et al.*, 2010; Cheng *et al.*, 2013; Bahuguna & Jagadish, 2015), the outcome of which is a reduction in vegetative plant growth (Quint *et al.*, 2016), impacts on flower development and fertility (Balasubramanian *et al.*, 2006; Koini *et al.*, 2009; McClung & Davis, 2010), and the inhibition of plant defense signaling in response to a range of biotic threats (Wang

& Hua, 2009; Wang *et al.*, 2009). Not surprisingly, plants have evolved mechanisms to cope with simultaneous exposure to biotic and abiotic stress, and in this they utilize overlapping mechanisms not only to respond to stress but also to anticipate environmental changes for the purpose of regulating the timing and amplitude of seemingly opposing signaling processes (Quint *et al.*, 2016; Gimenez *et al.*, 2018; Saijo & Loo, 2020; Iqbal *et al.*, 2021).

As a point of convergence with biotic stress signaling, changes in the abiotic environment have been shown to profoundly impact the plant immune system, including the activation, duration, and attenuation of signaling (Venkatesh & Kang, 2019). Indeed, recent studies have demonstrated that the function of at least two key nodes of the plant immune system – namely, pathogen-associated molecular-pattern-triggered immunity (PTI) and effector-triggered immunity (ETI) – are intimately associated with processes required for response to abiotic stress (Tsuda *et al.*, 2009). ETI, which is manifested following the recognition of pathogen race-specific avirulence (Avr) proteins (aka, effectors), is regulated by host-plant-derived resistance (R) genes (Jones & Dangl, 2006; P. Li *et al.*, 2020; Z. Li *et al.*, 2020). As a highly conserved family of proteins

found in all plants, nucleotide-binding leucine-rich repeat (NB-LRR) protein molecules mediate the specific recognition of pathogens via the indirect and/or direct recognition of both conserved and race-specific virulence factors (Elmore *et al.*, 2011).

In addition to NB-LRR proteins, numerous additional processes have been identified as critical components of the immune signaling network (De Vleeschauwer *et al.*, 2014; Tsuda & Somssich, 2015; Li & Day, 2019; Maier *et al.*, 2021). Interestingly, research has also demonstrated a role for these (i.e. phytohormones, transcription factors) in abiotic stress signaling (Berens *et al.*, 2019; Saijo & Loo, 2020). Among these, *NON-RACE-SPECIFIC DISEASE RESISTANCE-1* (*NDR1*) was identified nearly three decades ago as a critical component of plant immune system function (Century *et al.*, 1995), with key functions associated with ETI and salicylic acid (SA)-dependent, signaling networks in Arabidopsis (Lu, 2009; Lu *et al.*, 2013). As a broader role for *NDR1* in plant processes, recent work has shown that *NDR1* and *NDR1*-like genes (i.e. *HIN*; Bao *et al.*, 2016) play important roles in stress response signaling (Lu *et al.*, 2021). Among the best characterized examples of *NDR1*-dependent immune signaling cascades is *RESISTANCE TO PSEUDOMONAS SYRINGAE-2* (*RPS2*) (Kunkel *et al.*, 1993), an NB-LRR-encoding gene required for the recognition and activation of resistance in response to the Gram-negative bacterial phytopathogen *Pseudomonas syringae* expressing the type III effector (T3E) protein *AvrRpt2*. Cleavage of RPM1-interacting protein 4 (*RIN4*) by *AvrRpt2* is required for the activation of *RPS2*-based ETI (Mackey *et al.*, 2003). In the absence of *RPS2*, *AvrRpt2* promotes pathogen virulence in host cells (Mudgett, 2005). As a function for the role of *NDR1* in *RPS2* signaling, previous work demonstrated that *RPS2*-mediated resistance is *NDR1* dependent (Axtell *et al.*, 2003). Furthermore, enhanced level of disease resistance has been observed in the *NDR1*-overexpression line (Coppinger *et al.*, 2004), indicating cleavage of *RIN4* by *AvrRpt2* would occur more rapidly in this line, thereby leading to the release of negative regulation on the R-proteins *RPS2* (Axtell & Staskawicz, 2003) and *RPM1* (Mackey *et al.*, 2003) and the subsequent activation of ETI.

Herein, we describe a role for *NDR1* in plant immunity under heat stress conditions. Using a combination of physiological and transcriptome-based approaches, we observed that in contrast to the temperature-sensitive SA defense pathway gene *ISOCHRISMATE SYNTHASE 1* (*ICS1*) (Huot *et al.*, 2017), the *NDR1*-overexpression line stabilizes ETI-specific *RPS2* messenger RNA (mRNA) accumulation at elevated temperature. Our findings suggest pathogen resistance at elevated temperature is mediated through crosstalk between *NDR1* and *RPS2*, a mechanism that requires robust signaling of SA-dependent processes.

Materials and Methods

Plant material and growth conditions

Arabidopsis thaliana (L.) Heynh. seeds ecotype Columbia-0 (Col-0) were used as wild-type (WT) plants, together with mutant plants (*ndr1*, *ndr1/35S::NDR1*, and *ics1-2*), all of which are in the Col-0 background. Plants were grown in Arabidopsis soil mix comprised

of equal parts of Sure-Mix (Sure, Galesburg, MI, USA), Perlite (PVP Industries, Orwell, OH, USA), and Vermiculite (PVP Industries). Plants were grown for 3–4 wk at 21°C under a 12 h : 12 h, light : dark cycle with 60% relative humidity and a light intensity of 120 $\mu\text{mol m}^{-2} \text{s}^{-1}$ prior to heat stress in a BigFoot Series growth chamber (BioChambers, Winnipeg, MB, Canada). For temperature assays, plants were separated into two chambers set to either 21°C (permissive) or 29°C (elevated). Plants were subjected to heat stress treatment for 48 h at 29°C prior to pathogen treatment. The area of infiltration was marked to ensure that the leaf tissue subsequently collected for the assays contained bacterial inoculum.

Bacterial strains and disease assays

Pseudomonas syringae pv *tomato* (*Pst*) DC3000 harboring the open-reading frames of the T3E, *AvrRpt2*, *AvrPphB*, *AvrRpm1*, as well as the empty vector (EV; pVSP61; Kunkel *et al.*, 1993) were grown on NYGA (5 g l⁻¹ Bacto-peptone, 3 g l⁻¹ yeast extract, and 20 ml l⁻¹ glycerol, with 15 g l⁻¹ agar for solid medium) containing 25 $\mu\text{g ml}^{-1}$ kanamycin (kan) and 100 $\mu\text{g ml}^{-1}$ rifampicin (rif) for 2 d at 28°C. After 48 h, bacterial cultures were resuspended in 5 mM magnesium chloride (MgCl₂) at the desired concentrations for *in planta* growth assays. The same growing and culture suspension method was followed for the adenylate cyclase (*CyaA*) fusion-protein-tagged variant of *AvrRpt2* and type-III secretion system (T3SS) mutant *hrcC*⁻, with the exception that NYGA plates contained 25 $\mu\text{g ml}^{-1}$ rif and 10 $\mu\text{g ml}^{-1}$ gentamycin (gen).

In planta bacterial growth assays

Pst harboring *AvrRpt2*, *AvrPphB*, *AvrRpm1*, and EV (control) inoculums were prepared at an optical density at 600 nm $\text{OD}_{600 \text{ nm}} = 0.0005$ (5×10^5 CFU ml⁻¹), $\text{OD}_{600 \text{ nm}} = 0.1$ (10^8 CFU ml⁻¹) and $\text{OD}_{600 \text{ nm}} = 0.0075$ (7.5×10^6 CFU ml⁻¹) for growth curve, hypersensitive response (HR), and benzothiadiazole (BTH) assays, respectively. Bacterial inoculations were performed on multiple ($n > 3$) fully expanded leaves from 3-wk-old Arabidopsis plants grown at permissive (21°C) and elevated (29°C) temperatures. Plants were inoculated with *Pst* isolates using a needleless syringe. Three biological replicates were performed for each assay. For *in planta* bacterial growth curve analyses, 3 mm leaf disks from three plants (three leaves per sample) were collected at 3 d after inoculation (DAI). Harvested leaf discs were incubated in 5 mM MgCl₂ + 0.1% Tween-20 at 28°C, on a rotary platform shaker, for 1 h. After 1 h, each sample was serially diluted (10-fold increments) and 5 μl of each dilution was plated on NYGA plates containing half-strength antibiotics (i.e. rif and kan). After 2 d incubation at 28°C, bacterial CFUs were counted. For HR analysis, infected leaves (24 h post-inoculation (hpi)) were collected, and phenotypes were recorded by digital photography.

RIN4 Western blot analysis

Two leaves from each plant genotype were hand infiltrated ($\text{OD}_{600 \text{ nm}} = 0.1$; $c. 10^8$ CFU ml⁻¹) with *Pst* expressing either

AvrRpt2 or EV. Infiltrated leaves were collected at the designated timepoints, placed into a sterile 2 ml centrifuge tube, and were flash frozen in liquid nitrogen (N₂). Samples were ground in extraction buffer (20 mM Tris pH 7.5, 150 mM sodium chloride, 1 mM EDTA, % Triton X-100, 0.1% sodium dodecyl sulfate (SDS), 5 mM dithiothreitol (DTT), 10× Sigma protease inhibitor mixture) and centrifuged at 20 000 *g* for 10 min at 4°C. After centrifugation, the supernatant was collected as the total protein extract. Total protein of 50 µg was equalized using 6× loading buffer (0.375 M Tris pH 6.8, 12% SDS, 60% glycerol, 0.6 M DTT, 0.06% bromophenol blue) as a dilutant. Samples were separated by SDS polyacrylamide gel electrophoresis using 4–12% NuPAGE gels (Invitrogen) followed by transfer onto nitrocellulose membranes (GVS North America, Sanford, ME, USA) for Western blot analysis.

Polyclonal rabbit anti-RIN4 antibody was produced by Cocalico Biologicals Inc. (Stevens, PA, USA). The specificity of anti-RIN4 antibody was confirmed by Western blot analysis using WT Col-0 and *rps2/rin4* mutant plant lines, as well as transient expression of RIN4 protein in *Nicotiana benthamiana*. Anti-RIN4 sera was used at a concentration of 1 : 5000 in 1× TBST (1 M Tris pH 8.0, 1% Tween 20, 5% dehydrated milk).

Phytohormone analysis

Leaves were infiltrated with *Pst* suspended in 5 mM MgCl₂ expressing AvrRpt2, AvrRpm1, or *Pst* harboring pVSP61 (EV) using a 1 ml needleless syringe at a concentration of OD_{600 nm} = 0.0005. Mock inoculation controls were performed using 5 mM MgCl₂. Quantification of phytohormones was performed as previously described (Velasquez *et al.*, 2017), with minor modifications. For hormone extraction and quantitative evaluation, frozen tissue was ground using a TissueLyser II (Qiagen) and incubated on a rocking platform at 4°C for 24 h in extraction buffer (80 : 20 v/v HPLC-grade methanol : water with 0.1% formic acid (v/v), 0.1 g l⁻¹ butylated hydroxytoluene). Samples were centrifuged at 12 000 *g* for 10 min at 4°C, and the resultant supernatants were collected and filtered through a 0.2 µm polytetrafluoroethylene membrane (Millipore).

Abscisic acid (ABA)-*d*₆ (Toronto Research Chemicals Inc., North York, ON, Canada) served as an internal standard. Injections of plant extracts (10 µl per injection) were separated on a Waters Acquity BEH-C18 column (2.1 mm × 50 mm, 1.7 µm) installed in the column heater of an Acquity ultraperformance liquid chromatography system (Waters Corp.). A gradient of 0.1% aqueous formic acid (solvent A) and methanol (solvent B) was applied in a 5 min program with a mobile phase flow rate of 0.4 ml min⁻¹ as follows: 0–0.5 min hold at 98% A and 2% B, transition to 70% B at 3 min, to 99% B at 4 min, hold at 99% B to 5 min, return to 98% A at 5.01 min and hold at 98% A to 6 min. The column was maintained at 40°C and interfaced to a Waters Xevo TQ-XS mass spectrometer equipped with electrospray ionization and operated in negative-ion mode with a capillary voltage of 1.00 kV. The flow rates of cone gas and desolvation gas were 150 and 800 l h⁻¹, respectively. The source temperature was 150°C, and the desolvation temperature was

400°C. Collision energies and source cone potentials were optimized for each compound using QUANOPTIMIZE software (Waters Corp.). Peak areas were integrated, and the analytes were quantified based on standard curves generated from peak area ratios of analytes. Data acquisition and processing were performed using MASSLYNX 4.1 software (Waters Corp., Milford, MA, USA). Analytes were quantified by converting peak area to phytohormone concentration (nanomolar) per gram of DW of leaf tissue using a standard curve specific to each compound.

Adenylate cyclase assay

To monitor *Pst* type-III effector delivery, a CyaA assay was performed as previously described (Fu *et al.*, 2006; Chakravarthy *et al.*, 2017), with slight modification. In brief, leaves from 4-wk-old Arabidopsis plants were infiltrated with *Pst* expressing AvrRpt2-CyaA or the T3SS mutant *hrcC*⁻ carrying AvrRpt2-CyaA suspended in 5 mM MgCl₂ at a concentration of OD_{600 nm} = 0.005 (*c.* 5 × 10⁶ CFU cm⁻¹) using a 1 ml needleless syringe. Leaf samples were harvested from two plants (two leaves per sample) at 0, 6, and 10 hpi and snap frozen in liquid N₂. Cyclic adenosine monophosphate (cAMP) levels were quantified using the direct cAMP ELISA kit (ADI-900-066; Enzo Life Sciences, Farmingdale, NY, USA).

RNA extraction, library preparation, and RNA sequencing

RNA sequencing (RNA-seq) analyses were performed on Arabidopsis plants representing four genotypes: WT Col-0, *ndr1*, *ndr1/35S::NDRI*, and *ics1-1*. Plants were grown at permissive temperatures (i.e. 21°C) for 23 d and then moved to elevated (i.e. 29°C) temperatures. Upon moving to 29°C, two fully expanded leaves from four different plants (eight leaves) were harvested as a single biological replicate at 0, 6, and 24 h. Tissue isolations were collected from three independent experimental replications, each containing three biological replicates. Total RNA was extracted using the RNeasy Plant Mini kit (Qiagen). DNA was removed from the sample by using a TURBO DNA-Free™ kit (Thermo-Fisher, Waltham, MA, USA). RNA samples were quantified using a Nanodrop 2000 spectrophotometer (Thermo-Fisher).

Construction of strand-specific RNA-sequencing libraries

Construction of the RNA-seq libraries and sequencing on the Illumina NovaSeq 6000 were performed at the Roy J. Carver Biotechnology Center at the University of Illinois at Urbana-Champaign. Total RNAs were run on a fragment analyzer (Agilent, Santa Clara, CA, USA) to evaluate RNA integrity. RNA-seq libraries were constructed with the TruSeq Stranded mRNAs Sample Prep kit (Illumina, San Diego, CA, USA). Polyadenylated mRNAs were enriched from 500 ng of high-quality DNA-free total RNA with oligo-dT beads. The final libraries were quantitated using Qubit (Thermo-Fisher), and the average library fragment length was determined on a fragment analyzer. The libraries were diluted to 10 nM and further quantitated by quantitative PCR (qPCR) on a CFX Connect Real-Time qPCR system (Bio-Rad) for accurate pooling of the barcoded libraries and

maximization of number of clusters in the flow cell. A total of 90 RNA-seq libraries were prepared from 1 µg of total RNA.

Sequencing of libraries on the NovaSeq instrument

The pooled barcoded RNA-seq libraries were loaded on a NovaSeq S2 lane for cluster formation and sequencing. Sequencing was performed by the Roy J. Carver Biotechnology Center at the University of Illinois, Urbana-Champaign. Libraries were sequenced from one end of the fragments for a total of 100 nt. The FASTQ read files were generated and demultiplexed with the BCL2FASTQ v.2.20 conversion software (Illumina).

Expression and differential analysis

The adapter sequences and low-quality bases ($q < 10$) were trimmed by TRIMMOMATIC (Bolger *et al.*, 2014). Resultant cleaned reads were mapped to the TAIR10 reference genome using HISAT2 (Kim *et al.*, 2015). Mapped read counts for each gene were generated using the HTSEQ (Anders *et al.*, 2015) command. The statistical analysis of the RNA-seq data was performed in the R environment (v.4.0.5). Mitochondrial and chloroplast genes were excluded from analysis. Genes with mean read counts of fewer than 10 per library were also excluded from analysis. The resulting count data were subjected to trimmed-mean of M -values normalization using the function calcNormFactors in the package EDGER, followed by log-transformation by the function voomWithQualityWeights in the package LIMMA to yield \log_2 counts per million. To each gene, a linear model was applied using the lmFit function in the LIMMA package with the following terms: $S_{getr} = \text{GET}_{get} + \varepsilon_{getr}$, where S is the \log_2 expression value, GET is the (genotype : environment : time) interaction, r is the biological replicate, and ε is the residual. For variance shrinkage in the calculation of P -values, the eBayes function in the LIMMA package was used. Next, the resulting P -values were corrected for multiple hypothesis testing by calculating the Storey q -values using the function qvalue in the package QVALUE. To extract genes with significant expression changes, the cutoff of q -value < 0.01 and greater than two-fold expression changes were applied. AGRIGO was used for Gene Ontology (GO) enrichment analysis with default settings (Du *et al.*, 2010). To create heatmaps, average linkage hierarchical clustering with uncentered Pearson correlation as a distance measure was carried out using CLUSTER 3.0 (Eisen *et al.*, 1998), followed by visualization using TREEVIEW (Eisen *et al.*, 1998).

Coexpression network analysis was performed using the R package WGCNA (Langfelder & Horvath, 2008). Genes with small expression variances (< 0.2) across the samples were excluded. Normalized and \log_2 -transformed read counts of the resulting 11 898 genes were used for constructing a signed hybrid network. The adjacency matrix was constructed using the adjacency function with the power of 14, and the topological overlap was then calculated from the adjacency matrix using the TOMsimilarity function. Average linkage hierarchical clustering was applied to the topological overlap for grouping genes with highly similar coexpression relationships. The Dynamic Hybrid Tree Cut

algorithm was used to cut the hierarchical clustering tree, and 37 modules were defined as branches from the tree cutting. For the construction of the NDR1-centered network, eigengene-based gene connectivity, kME, was calculated using the signedKME function to select coexpression modules whose expression patterns are highly correlated to that of NDR1 ($\text{lkME1} > 0.6$). The relationships of these modules with *NDR1* were visualized using CYTOSCAPE (Shannon *et al.*, 2003).

Results

Temporal dynamics of transcriptome responses to heat stress through NDR1-dependent immune activation

The loss of *NDR1* has a profound impact on pathogen defense signaling and disease resistance in plants (Century *et al.*, 1995). Previous results suggest that one mechanism underpinning this activity may intersect with broader stress response processes, including those associated with plant hormone-based signaling and the maintenance of cellular integrity (Knepper *et al.*, 2011). To define how *NDR1* influences plant response to abiotic stress response, we first conducted a comprehensive RNA-seq analysis over a 24 h period following permissive temperature (i.e. 21°C) and heat stress (i.e. 29°C) exposure in WT Col-0, the *ndr1* mutant, a previously characterized *ndr1/35S::NDR1*-overexpression line (Coppinger *et al.*, 2004), and the SA-deficient mutant *ics1-2*. The impetus for this was to determine the rapid transcriptional responses required for signaling in response to pathogen infection and elevated temperature, as well as to define the potential priming of immune responses and their relationship to heat tolerance.

Hierarchical clustering analysis of 11 245 differentially expressed genes (DEGs) revealed gene expression changes over the 24 h time course across all genotypes (Fig. 1a; Supporting Information Table S1). Further analysis identified two significant gene clusters that showed significant response(s) to heat stress. The first, cluster 1, contains 800 genotype-independent temperature-responsive genes (Figs 1a, S1; Tables S2, S3). As revealed by GO enrichment analysis, this cluster contains a large number of genes involved in mitochondrial RNA editing, suggesting the role of mitochondrial RNA editing in acclimation to high temperature. This is supported by a recent paper reporting that an Arabidopsis mutant lacking the mitochondrial RNA editing enzyme GEND1 is hypersensitive to high temperature (Guo *et al.*, 2021). Notably, cluster 2, which is comprised of 2151 genes, is enriched in transcripts that were highly expressed in the *NDR1*-overexpression line (*ndr1/35S::NDR1*) and are related to defense response and immune system function based on GO enrichment analysis (Fig. 1c; Tables S4, S5). Interestingly, following 24 h exposure to elevated temperature, *NDR1*-overexpressing plants had the greatest number of DEGs, up or downregulated, compared with *ndr1* and *ics1-2* (with WT Col-0 as a baseline) (Fig. 1b; Tables S6, S7).

To further evaluate how the *NDR1* overexpression line maintains enhanced immune responses at elevated temperature, we next examined *NDR1*-dependent and independent DEGs under heat stress. *NDR1*-dependent genes were selected as DEGs that

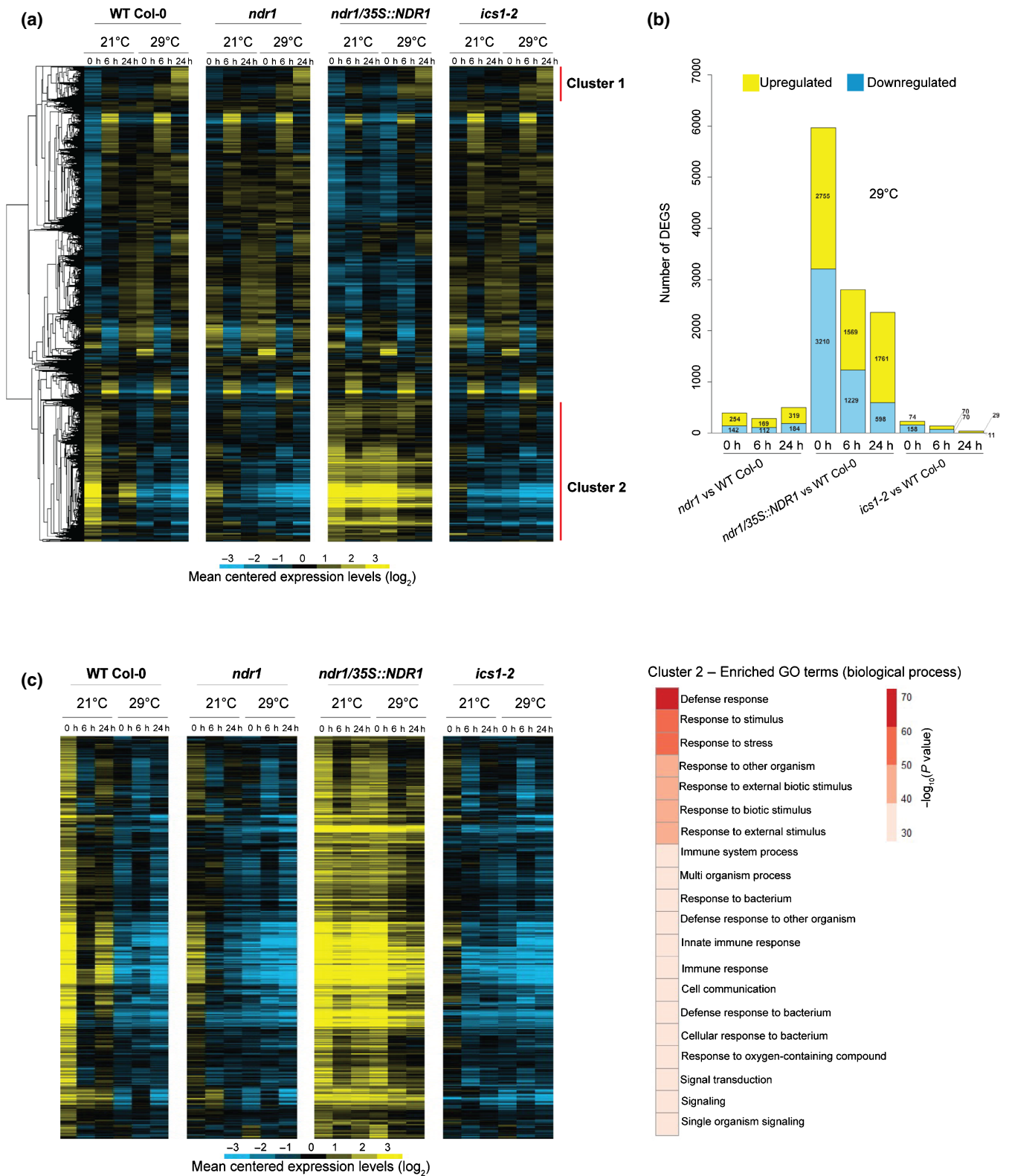


Fig. 1 Temporal dynamics of transcriptome responses to heat stress through Non-Race-Specific Disease Resistant1 (NDR1)-dependent immune activation in *Arabidopsis*. (a) Heat map showing \log_2 -fold gene expression changes over the 24 h heat stress. (b) Number of differentially expressed genes (DEGs) at 29°C over a 24 h time course in the *ndr1*, *NDR1*-overexpression, and *ics1-2* mutant plants. (c) Heat map showing \log_2 -fold gene expression changes in cluster 2 genes that are highly expressed in *ndr1/35S::NDR1* plants and are related to defense response and immune system based on Gene Ontology (GO) enrichment analysis. Blue indicates negative values, yellow indicates positive values, and black indicates zero.

were upregulated (*NDR1*-up) or downregulated (*NDR1*-down) in *ndr1/35S::NDR1* plants compared with WT Col-0 after the exposure to elevated temperature at 29°C ($q < 0.01$ and $\log_2FC > 1$ or < -1). Heat-responsive genes were selected as DEGs that were induced (heat-induced) or suppressed (heat-suppressed) in WT Col-0 exposed to elevated temperature at 29°C compared with WT Col-0 grown at 21°C ($q < 0.01$ and $\log_2FC > 1$ or < -1). As shown in Fig. S2, a large portion of heat-suppressed genes overlap *NDR1*-up genes at both 6 and 24 h. Similarly, there is a substantial overlap in the gene lists between *NDR1*-down and heat-induced genes. These results further support our claim that *NDR1* overexpression maintains the expression of genes that are otherwise vulnerable to heat. Not surprisingly, little overlaps were found between *NDR1*-up and heat-induced genes and between *NDR1*-down and heat-suppressed genes, suggesting that *NDR1* overexpression has little effect on the regulation of heat-responsive genes (Tables S8–S11). Furthermore, GO terms ‘defense response’ and ‘response to salicylic acid’ are found in genes that are upregulated in *NDR1*-overexpression line but suppressed by heat stress at both 6 and 24 h (Tables S12–S15). This further supports that *NDR1* overexpression protects defense-related genes from perturbation by heat. Genes that are suppressed in *NDR1*-overexpression line but induced by heat at 6 h are associated with ‘response to water/ABA’. Taken together, overexpression of *NDR1* imparts a pre-emptive activation of immunity by heat stress.

Overexpression of *NDR1* results in sustained accumulation of *RPS2* messenger RNA

The data described so far herein support a role for transcriptional induction of defense responses in the *NDR1*-overexpression line at elevated temperature. This is exciting, as it points to a possible intersection between immunity and elevated temperature response through *NDR1*, a key regulator of ETI-based immune activation and signaling. To gain insight into the role of *NDR1* at the intersection of immunity and high-temperature response, we performed a coexpression network analysis using the R package WGCNA. This approach led to the identification of 37 modules with distinct expression patterns, as indicated by module eigen-genes (MEs), which summarized the expression levels of the corresponding modules (Fig. S3). Using this, we calculated correlations of the expression pattern of *NDR1* and those of MEs. From this, we selected correlated modules (|correlation coefficient| > 0.6) to construct an *NDR1*-centered coexpression network (Fig. 2a). Within this network, *NDR1* showed positive and negative correlations with modules 1 and 6 and modules 2 and 4, respectively. Modules 1 and 6 showed upregulation in the *NDR1*-overexpression line, and this upregulation was maintained at elevated temperature (Fig. 2b). Further, these modules were enriched for genes associated with immunity-related GO terms, such as ‘defense response’ and ‘innate immune response’ (Fig. 2a; Tables S16, S17). By contrast, modules 2 and 4 showed heat-resistant downregulation in the *NDR1*-overexpression line and were enriched for genes associated with photosynthesis and growth-related GO terms (Fig. 2a; Tables S16, S17). The output

of this analysis revealed that *NDR1* overexpression activates defense-associated gene expression and protects these expression networks from perturbation by elevated temperature.

NDR1 is required for the activation of ETI through a defined set of NB-LRR R-proteins (e.g. *RPS2*, *RPM1*) (Day *et al.*, 2006; van Wersch *et al.*, 2020). Previous studies showed that *RPS2* is required for *Psm* ES4326 AvrRpt2 and *Pto* DC3000 AvrRpt2-induced SA accumulation and the induction of immune-associated transcripts (Liu *et al.*, 2016; Mine *et al.*, 2018). Interestingly, we found that *RPS2* is included in module 6 (i.e. heat-resistant upregulation) in the *NDR1*-overexpression line. Based on this, we further evaluated the mRNA accumulation of *RPS2* and other key defense-associated genes at both permissive (21°C) and elevated (29°C) temperatures (Figs 2c, S4). In contrast to the other genotypes, the downregulation of the R proteins *RPS2*, *RPM1*, and *RPS1* together with *NDR1* (control) at 24 h was not observed in the *NDR1*-overexpression line at elevated temperature (Fig. 2c; Table S1). Expression of the key genes in SA response, *ICS1*, *CALMODULIN BINDING PROTEIN 60g* (*CBP60g*), and *PATHOGENESIS RELATED GENE 1* (*PR1*) was reduced at elevated temperature, but still higher in the *NDR1*-overexpression line than in the other genotypes (Fig. S4). The gene expression level changes observed at T_0 in all genotypes at 21°C and 29°C is likely due to occur through a combination of factors, such as the function of the genes themselves, changes occurring in response to the transfer of plants from permissive to elevated temperature chamber, and/or due to wounding during sampling.

To further define *NDR1*'s role as a regulator of general stress response signaling in Arabidopsis, we next asked if *NDR1* is required for disease resistance signaling at elevated temperature. To do this, we first evaluated the activation of immune signaling in response to simultaneous exposure of elevated temperature and pathogen infection. Consistent with the requirement for *NDR1* in the activation of *RPS2*-mediated ETI, WT Col-0 and *ndr1/35S::NDR1*, but not *ndr1*, responded to *Pst*-AvrRpt2 with rapid induction of the HR at both permissive and elevated temperatures (Fig. 3a, top two panels). This result was consistent with the absence of disease symptoms in WT Col-0 and the *NDR1*-overexpression line, and the development of disease symptoms (e.g. chlorosis) (Fig. 3a, lower two panels) in both the *ndr1* and *ics1-2* mutants. As a further confirmation of this interaction, we also evaluated the *in planta* bacterial growth at 3 DAI to examine the level of host resistance and/or susceptibility against *Pst* DC3000 (*Pst*) and *Pst*-AvrRpt2. As shown, and consistent with the results of the HR assay, we observed enhanced susceptibility in plants lacking *NDR1* (*ndr1*) and SA (*ics1-2*), whereas WT Col-0 and *ndr1/35S::NDR1* showed resistance at elevated temperature (Fig. 3b). *In planta* bacterial growth at 0 hpi was also quantified to capture any population-dependent growth rate differences (Fig. S5). Collectively, these results demonstrate that key regulators of SA, as well as the expression of *NDR1*-dependent resistance signaling (e.g. *RPS2*), are enhanced in the *NDR1*-overexpression line at elevated temperature.

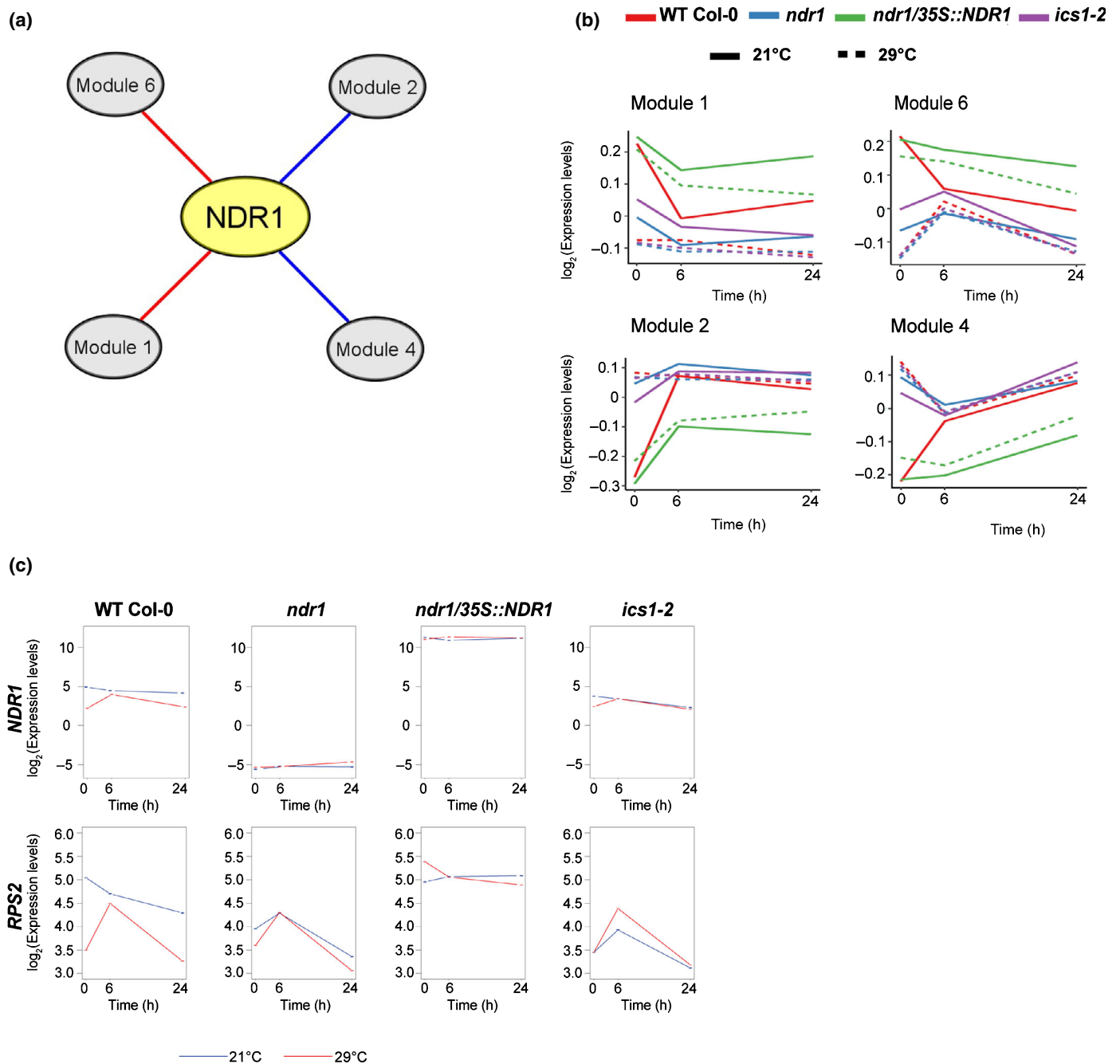


Fig. 2 NON-RACE-SPECIFIC DISEASE RESISTANCE1 (*NDR1*) overexpression in *Arabidopsis* induces expression of immunity genes and protects it from perturbation by elevated temperature. (a) An *NDR1*-centered coexpression network reveals modules whose expression levels are correlated at elevated temperature in the *NDR1*-overexpression line. Red and blue edges indicate positive and negative correlation, respectively. (b) Averaged expression levels of genes in the modules summarized by module eigengenes. (c) Overexpression of *NDR1* results in sustained accumulation of *RESISTANCE TO PSEUDOMONAS SYRINGE-2* (*RPS2*) messenger RNA at both 21°C and 29°C.

Pst-AvrRpt2 promotes effector-triggered immunity-induced salicylic acid accumulation at elevated temperatures

To determine if the observed disease resistance phenotype in the *NDR1*-overexpression line following challenge with avirulent *Pst*-AvrRpt2 is mediated by SA at elevated temperatures, we quantified the level of SA in plants hand-infiltrated with *Pst* and *Pst*-

AvrRpt2 at 24 hpi. Consistent with previous reports, we observed a decreased SA accumulation at elevated temperature, compared with those at permissive temperature (21°C), following mock and *Pst* treatment (Fig. 4a,b) (Huot *et al.*, 2017). Intriguingly, we found that ETI triggered by *Pst*-AvrRpt2 led to a significant increase in the levels of SA in WT Col-0 (Fig. 4c). In addition, the SA levels in the *ndr1/35S::NDR1*-overexpression line remained stable, in comparison with plants inoculated with

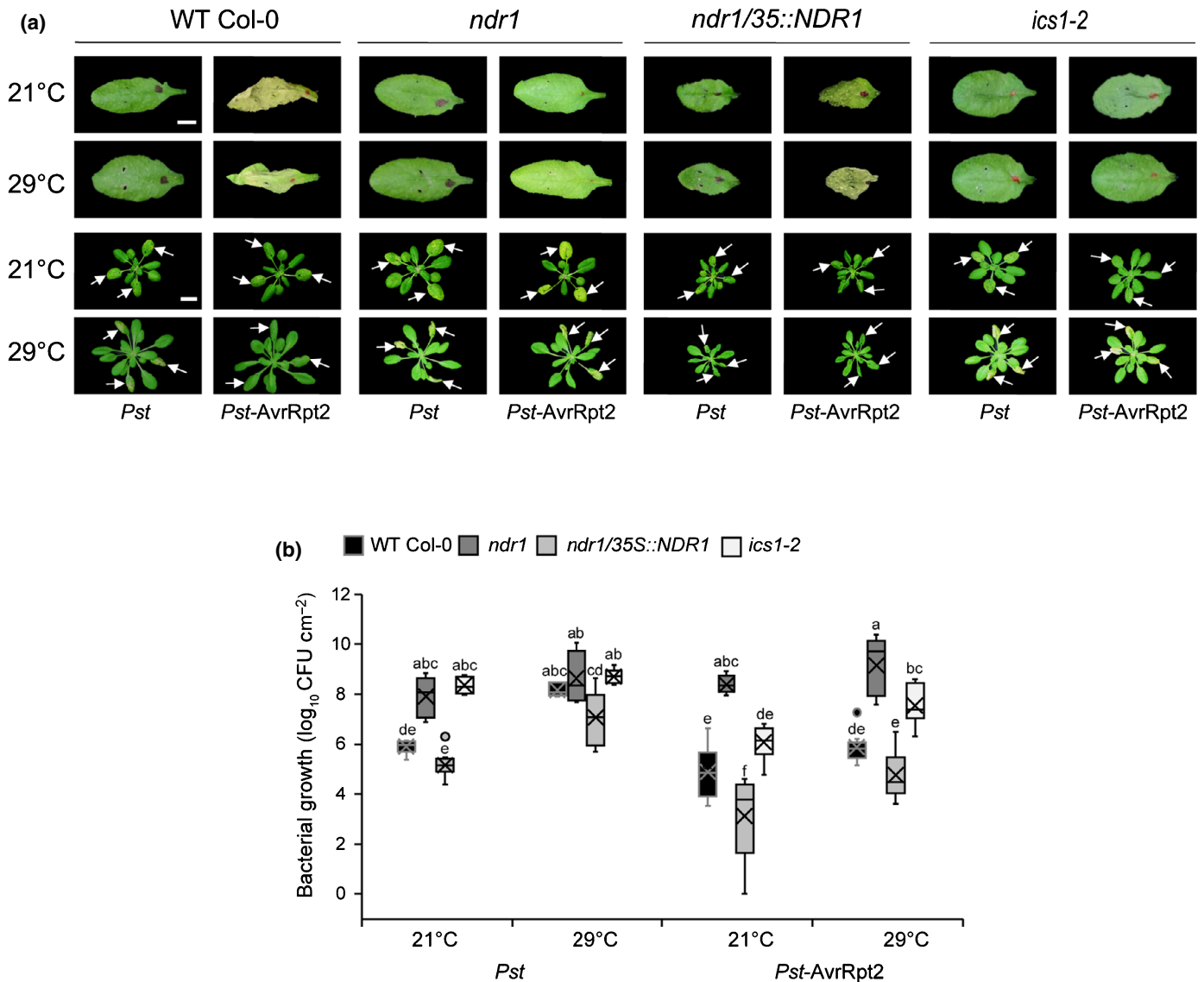


Fig. 3 Disease resistance at elevated temperature is linked to stable *RESISTANCE TO PSEUDOMONAS SYRINGAE-2 (RPS2)* messenger RNA expression in *ndr1/35S::NDR1* *Arabidopsis* plants. (a) Hypersensitive response at 24 h post-infection ($\text{OD}_{600 \text{ nm}} = 0.1$) (upper panel) and disease symptoms ($\text{OD}_{600 \text{ nm}} = 0.0005$) at 3 d post-inoculation (lower panel) at 21°C and 29°C. White arrows indicate leaves infiltrated. (b) Bacterial growth at 3 d after syringe-infiltration with *Pseudomonas syringae* pv *tomato* (*Pst*) and *Pst-AvrRpt2* ($\text{OD}_{600 \text{ nm}} = 0.0005$) in wild-type (Col-0) and mutant plants at 21°C and 29°C. *n* represents the total number of leaves from three independent biological repeats (*n* = 9). Values are plotted as boxplots split by the median, and the whiskers show the range of data. Different letters represent a significant difference at *P* < 0.05 with Tukey's honest significant difference (HSD) test. Bar, 0.5 cm. All data are representative of three independent experiments.

the virulent pathogen *Pst* at elevated temperature (Fig. 4c). The low levels of SA in the *ndr1* and *ics1-2* mutant plants are consistent with the observed susceptibility to *Pst-AvrRpt2* at both permissive and elevated temperatures (Fig. 3b).

To determine if overexpression of *NDR1*, and/or *Pst-AvrRpt2* infection, is responsible for the induction of SA at elevated temperature, we first evaluated the *in planta* bacterial growth in plants infiltrated with *Pst-AvrRpt2* and the *AvrRpt2* cysteine protease mutant *AvrRpt2*^{C122A} (Kim *et al.*, 2005). As expected, in the absence of the cysteine protease activity of *AvrRpt2* (e.g. *Pst* alone or *AvrRpt2*^{C122A}), we observed the absence of HR elicitation and the development of pronounced disease phenotypes in all plant lines at both

permissive and elevated temperatures (Fig. 4d,e). Next, to define the link between the cysteine protease activity of *AvrRpt2* and the induced accumulation of SA, we quantified the level of SA in WT Col-0 and the *NDR1*-overexpression plants at 24 hpi with *Pst-AvrRpt2*^{C122A}. In contrast to elevated levels of SA in plants following *Pst-AvrRpt2* infection, we observed low levels of SA at elevated temperature in WT Col-0 and *NDR1*-overexpression plants following *AvrRpt2*^{C122A} inoculation (Fig. 4f). Coupled with the aforementioned results (Fig. 4c), these data support a role for *Pst-AvrRpt2*-associated temperature-independent SA levels in WT Col-0 or the *NDR1*-overexpression plants grown at elevated temperatures. Based on this, we

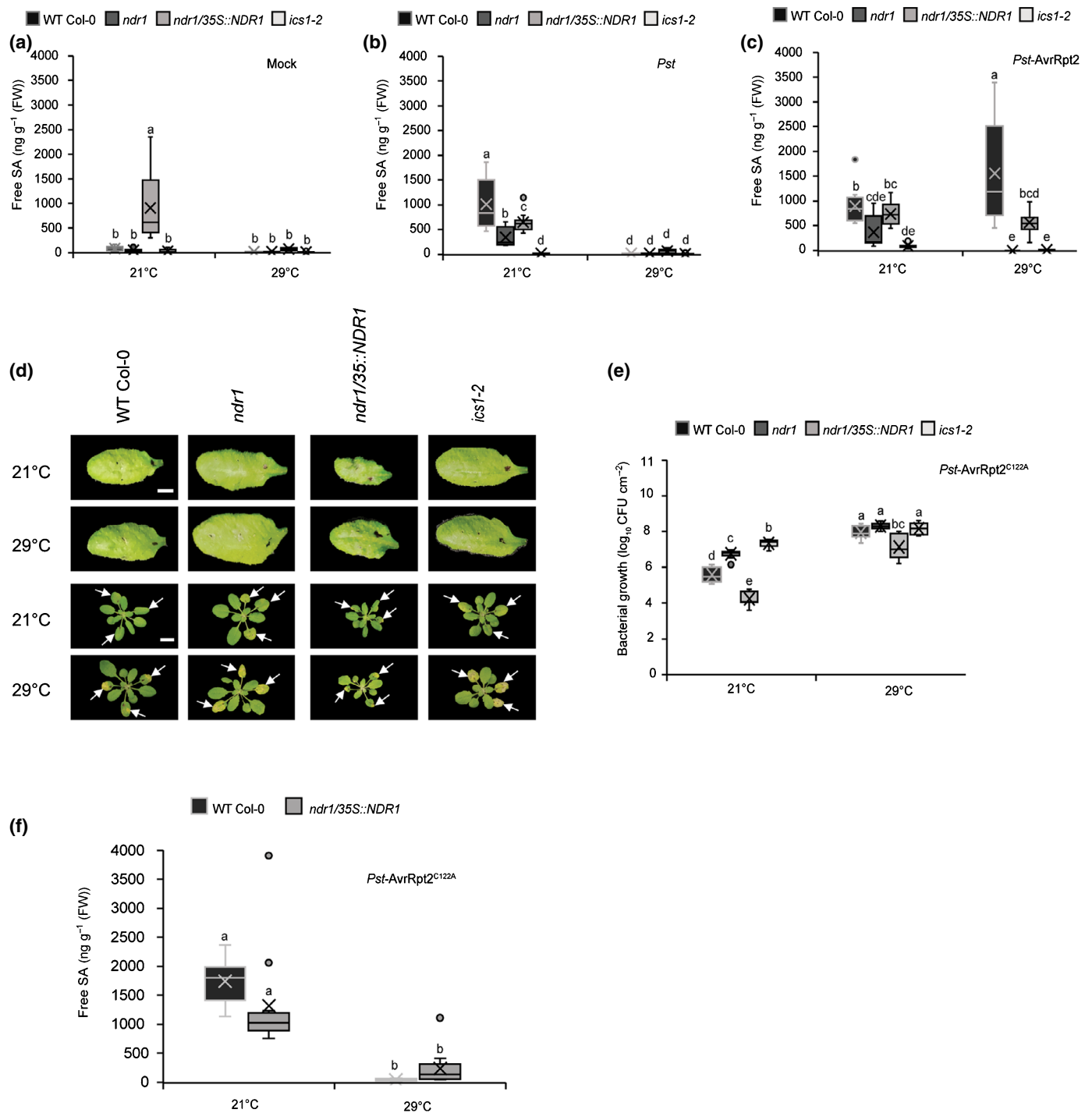


Fig. 4 *Pseudomonas syringae* pv *tomato* (*Pst*)-*AvrRpt2* promotes effector-triggered-immunity-induced salicylic acid (SA) synthesis in *Arabidopsis* at elevated temperature. (a) Basal accumulation of total SA in wild-type (Col-0) and mutant plants. Leaves of mock infiltrated plants were harvested at 24 h post-infection and evaluated for SA content. (b) Pathogen-induced SA levels in wild-type (Col-0) and mutant plants treated with *Pst* and (c) *Pst-AvrRpt2* ($OD_{600\text{ nm}} = 0.0005$). Leaves of pathogen-infiltrated plants were harvested at 24 h post-infection for SA quantification. (d) Hypersensitive response at 24 h post-inoculation ($OD_{600\text{ nm}} = 0.1$) (upper panel) and disease symptoms ($OD_{600\text{ nm}} = 0.0005$) at 3 d post-inoculation (lower panel) after syringe-infiltration with *Pst-AvrRpt2*^{C122A} in wild-type (Col-0) and mutant plants. White arrows indicate leaves infiltrated. (e) Bacterial growth at 3 d after syringe-infiltration with *Pst-AvrRpt2*^{C122A} ($OD_{600} = 0.0005$) in wild-type (Col-0) and mutant plants. (f) Levels of free SA in wild-type (WT) Col-0 and *ndr1/35S::NDR1* plants treated with *Pst-AvrRpt2*^{C122A} ($OD_{600} = 0.0005$). *n* represent total number of leaves from three independent biological repeats (for hormone quantification and disease assays, *n* = 12 and 9, respectively). Measures are plotted as boxplots split by the median, and the whiskers show the range of data. Different letters represent a significant difference at $P < 0.05$ with Tukey's honest significant difference (HSD) test. Bar, 0.5 cm. All data are representative of three independent experiments.

hypothesize that the observed resistance at elevated temperature is mediated by *Pst*-AvrRpt2-induced SA production/stabilization, as well as through *NDR1* overexpression.

Overexpression of *NDR1* leads to enhanced stability of RIN4 in the presence of *Pseudomonas syringae* expressing *Pst*-AvrRpt2

To further define the mechanism(s) underpinning the observation of pathogen-induced SA and the sustained accumulation of SA at elevated temperatures in the *NDR1* overexpression line, we first investigated the activation of ETI through the *NDR1*–RIN4 signaling node. We first evaluated the activity of the T3E cysteine protease AvrRpt2, by examining its ability to cleave RIN4 (Axtell *et al.*, 2003; Chisholm *et al.*, 2005). To begin, we quantified the RIN4 protein levels of the untreated plants at both permissive and elevated temperatures. The RIN4 protein levels were similar at both temperatures, as shown in Fig. S4(a). Next, we observed a decrease in RIN4 protein stability over time in the presence of *Pst*-AvrRpt2 at both permissive and elevated temperatures in WT Col-0, as well as in the *ndr1* and *ics1-2* mutants (Fig. 5a). Interestingly, in the *ndr1/35S::NDR1*-overexpression line, we did not observe a reduction in RIN4 following infection with *Pst*-AvrRpt2, suggesting that overexpression of *NDR1* may protect RIN4 from cleavage. As expected, we observed no RIN4 disappearance following *Pst* inoculation over the same time frame (Fig. S6; Table S18).

To gain a comprehensive understanding of the role of *NDR1* in ETI at elevated temperature, we further conducted disease assays in WT Col-0, *ndr1*, *ndr1/35S::NDR1*, and *ics1-2* plants following infection with *Pst* expressing, individually, the T3Es AvrRpm1 or AvrPphB. As shown, we observed comparable disease resistance to *Pst*-AvrRpt2 following both T3E infections in the *NDR1*-overexpression line at elevated temperature (Figs S7, S8). Based on these data, we surmise that enhanced resistance in *ndr1/35S::NDR1* against T3Es may be the result of their respective R protein interactions – both genetic and potentially physical – with *NDR1*, as well as via a yet to be defined function for *NDR1* in SA-dependent signaling cascades.

To determine how overexpression of *NDR1* and the associated increase in SA might function in the activation of resistance, we next monitored the release of the negative regulation of immunity via the cleavage of RIN4 by the T3E cysteine protease AvrRpt2 (Axtell *et al.*, 2003). To do this, we first evaluated the translocation of AvrRpt2 into plant cells via the T3SS at 0, 6, and 10 h via the infection of plants with *Pst*-expressing AvrRpt2 fused to a CyaA reporter (i.e. AvrRpt2-CyaA). As a negative control for these experiments, we employed a T3SS mutant *brcC* carrying AvrRpt2-CyaA to ensure that detected *in planta* levels of CyaA arose via the action of a functional T3SS (Li *et al.*, 2017). Additionally, *in planta* bacterial levels at each time point were quantified to eliminate any population-dependent translocation rate errors (Fig. S9). Consistent with previous studies that evaluated the impact of elevated temperatures on T3E translocation (Huot *et al.*, 2017), we observed increased levels of cAMP at elevated temperature in all four

plant genotypes compared with plants grown at permissive temperatures (i.e. 21°C; Fig. 5b–e). However, at 10 h, we observed the lowest levels of cAMP at elevated temperature in the *NDR1*-overexpression line compared with WT Col-0, followed by *ics1-2* and *ndr1* mutants (Fig. 5b–e). These data are consistent with the increased stability of RIN4 in the *NDR1*-overexpression line (Fig. 5a) and support a role for *NDR1* in protecting RIN4 in the presence of *Pst*-AvrRpt2.

Previous work demonstrated that the plant defense inducer BTH induces pathogen resistance in an SA-dependent manner (Huot *et al.*, 2017; Kouzai *et al.*, 2018). To further uncouple the role of *NDR1* and SA as a function of pathogen T3E activity, we first evaluated the effect of BTH on AvrRpt2-CyaA effector translocation in plants grown at both permissive and elevated temperatures. At neither temperature did we observe a significant change in the level of cAMP following BTH treatment, with the exception for in the *ics1-2* line; we hypothesize that this is due to the low cAMP amount detected with mock treatment (Fig. S10a,b), which is likely due to subtle differences in buffer content (e.g. dimethyl sulfoxide). Indeed, the lower levels of cAMP observed in BTH-treated *ics1-2* plants is consistent with our observations presented in Fig. 5, wherein the amount of effector translocation was reduced in the *NDR1*-overexpression line, which also has increased levels of SA. These data agree with the results shown in Fig. 4(a), wherein mock-treated *NDR1*-overexpression lines also had elevated levels of SA. As a control for these assays, we also enumerated *in planta* bacterial levels at 0 hpi to eliminate any population-dependent translocation rate errors (Fig. S11a,b). Overall, this result suggests that lower translocation rates observed in the *NDR1*-overexpression line (Fig. 5d) could be a consequence of the elevated levels of SA in this line.

Having demonstrated the impact of SA on bacterial T3E translocation into the host cell, we next queried the role of SA on RIN4 cleavage by *Pst*-AvrRpt2, a function required for the robust activation of R-protein (e.g. RPS2)-mediated ETI (Axtell *et al.*, 2003) following T3E (i.e. AvrRpt2) delivery and recognition. At the onset of this line of investigation, our working hypothesis was that, given the enhanced level of resistance in the *NDR1*-overexpression line (Coppinger *et al.*, 2004), cleavage of RIN4 by AvrRpt2 occurs more rapidly in this line, thereby leading to the release of negative regulation on the R-proteins RPS2 (Axtell *et al.*, 2003) and RPM1 (Mackey *et al.*, 2003) and the robust activation of ETI. To test this, we first monitored the levels of RIN4 protein in BTH-treated plant lines hand-infiltrated with *Pst*-AvrRpt2. As shown in Fig. S10(c,d), exogenous application of BTH did not protect RIN4 from cleavage by AvrRpt2 in WT Col-0, nor in the *ndr1* or *ics1-2* mutants. However, similar to results observed in Fig. 5(a), overexpression of *NDR1* did result in enhanced protection of RIN4 from cleavage by *Pst*-AvrRpt2. Based on this result, we conclude BTH-induced SA does not protect RIN4 under *Pst*-AvrRpt2 treatment. Thus, the inability of SA to protect RIN4 from cleavage, coupled with the observed RIN4 protection in the *NDR1*-overexpression line, is likely due to the physical interaction, and stoichiometry of this association, between RIN4 and *NDR1*.

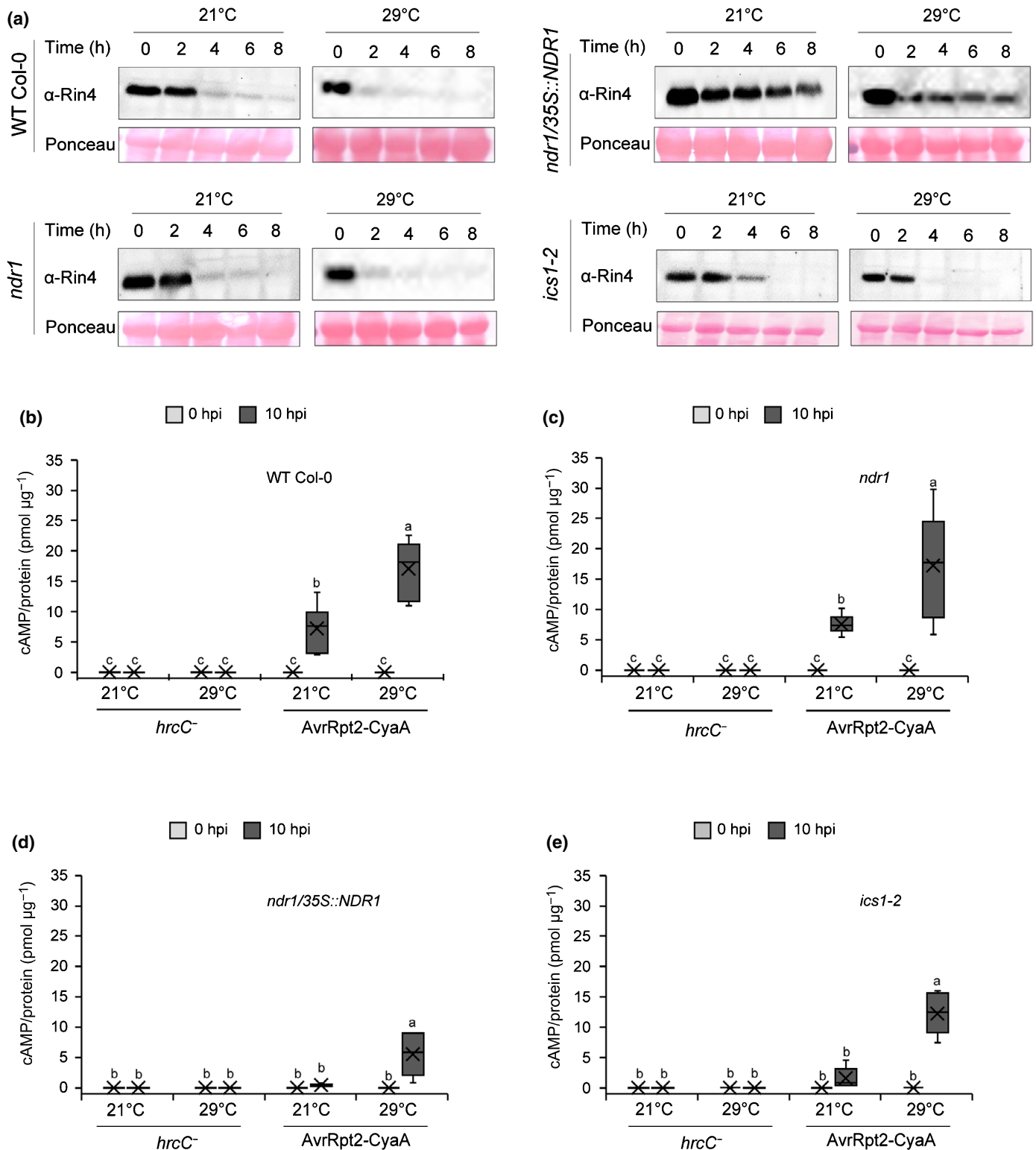


Fig. 5 *Pseudomonas syringae* pv *tomato* (Overexpression of *NON-RACE-SPECIFIC DISEASE RESISTANCE1* (*NDR1*) in *Arabidopsis* results in enhanced RPM1-interacting protein 4 (RIN4) stability in the presence of *Pst*-AvrRpt2. (a) Detection of RIN4 at 0, 2, 4, 6, and 8 h after syringe-infiltration with *Pst*-AvrRpt2 ($\text{OD}_{600 \text{ nm}} = 0.1$) in wild-type (Col-0) and mutant plants. The total protein extracts were subjected to -RIN4 Western blot. Equal loading of protein was verified by ponceau S staining of the membrane after protein transfer. (b–e) Effector translocation in *ndr1*, *ndr1/35S::NDR1*, and *ics1-2*, respectively, following syringe-infiltration with *Pst hrcC*⁻ or *Pst*-expressing AvrRpt2-CyaA ($\text{OD}_{600} = 0.005$). Tissue was collected at 0 and 10 h post-inoculation (hpi) for quantification of cyclic adenosine monophosphate (cAMP) which was normalized by total protein. Higher levels of cAMP indicate more translocation of bacterial effectors. *n* represents the total number of leaves from three independent biological repeats (*n* = 6). Values are plotted as boxplots split by the median, and the whiskers show the range of data. Different letters represent a significant difference at $P < 0.05$ with Tukey's honest significant difference (HSD) test. All data are representative of three independent experiments.

Discussion

Plant immune signaling during heat stress response has been described since the early 1900s, wherein it was demonstrated that the spread of tobacco mosaic virus necrotic lesions in *Nicotiana glutinosa*-infected leaves was more prevalent at elevated temperatures (Samuel, 1931). More than 75 yr after this discovery, similar correlations have been described as they relate to the impact of elevated temperature on plant growth (Penfield, 2008), reproduction (McClung & Davis, 2010), and hormone signaling (Sakata *et al.*, 2010). More recent work has shown that plant resistance to pathogens is reduced under conditions of elevated temperature, a phenomenon that is hypothesized to be associated with the downregulation of SA signaling (Li *et al.*, 2010; Huot *et al.*, 2017). Collectively, these studies have provided foundational support for the ‘growth–defense’ paradigm (Guo *et al.*, 2018). In the current study, to expand our understanding of the mechanisms that function at the nexus of heat stress response and immune signaling activation, we focused on the activation of a well-defined and genetically tractable immune signaling cascade, ETI.

Previous studies have shown that plant response(s) to both biotic and abiotic stimuli are initiated by rapid, highly specific, changes in the transcriptional landscape; notably, the induction of genes associated with plant defense (Hu *et al.*, 2012), and the attenuation of those required for growth and reproduction (Lee *et al.*, 2014; Quint *et al.*, 2016). These observations have led to the development of models that describe an important role for the co-regulation of processes that function antagonistically during simultaneous exposure to abiotic and biotic stressors (Hossain *et al.*, 2018; Kim *et al.*, 2020; Lu *et al.*, 2021). To dissect the role of elevated temperature on the activation of ETI, we generated 69 transcriptomes from four plant lines that have reported varied responses related to pathogen infection and hormone signaling, under permissive and elevated temperature (Century *et al.*, 1997; Tao *et al.*, 2003; Strawn *et al.*, 2007; Catinot *et al.*, 2008; Li *et al.*, 2021). Through this approach, we identified two main clusters of DEGs that segregated based on genotype-independent expression, as well as those that were regulated in a genotype-specific manner under elevated temperature. In the case of the latter, this cluster was comprised of highly expressed genes in the *NDRI*-overexpression line, many of which were related to GO terms including defense response and immune system function. Interestingly, our analysis revealed the stability of *RPS2* mRNA at elevated temperatures in the *NDRI*-overexpression line, a phenomenon we hypothesize is possibly attributable to downstream, preemptive, transcriptional activation of defense, and/or a consequence of elevated SA levels in the *NDRI* overexpressor. In either case, we posit that such a response would prime the immune system for protection during simultaneous biotic and abiotic stress exposure.

Phytohormones are an indispensable component of the plant immune system, required for the robust activation of both PTI and ETI (Miller *et al.*, 2017; Yuan *et al.*, 2021). Interestingly, SA production is also affected when plants are exposed to both low (P. Li *et al.*, 2020; Z. Li *et al.*, 2020) and elevated (Huot *et*

al., 2017) temperatures. As immune signaling modulators, previous work showed that *RPS2* is required not only for the production of SA, but also for the generation of pathogen-induced jasmonic acid and ABA production, supporting the hypothesis that, to some degree, defense hormone production is ETI dependent (Liu *et al.*, 2016). In contrast to published data showing loss of virulent *Pst*-induced SA biosynthesis at elevated temperature, we observed that avirulent *Pst*-AvrRpt2 promotes SA synthesis in a temperature-independent manner in WT Col-0 and the *NDRI*-overexpression line at 29°C (Huot *et al.*, 2017). Here, we observed that SA production was compromised in the *ndr1* mutant, similar to that in the SA-deficient *ics1-2* mutant line at elevated temperature. This is interesting; and with observed stability of *RPS2* mRNA at elevated temperature, high SA levels following *Pst*-AvrRpt2 treatment in the *NDRI*-overexpression line may be an underlying mechanism that contributes to reduced effector translocation.

Recent studies aimed at identifying the molecular–genetic mechanisms controlling immune signaling stability at elevated temperature have uncovered a relationship between an increase in temperature and the sustainable activity of host R-proteins (Venkatesh & Kang, 2019). For example, Arabidopsis plants subjected to a long-term (*c.* 10 d) temperature acclimation at 28°C resulted in an approximate eight-fold increase in the *in planta* growth at 3 DAI of the virulent pathogen *Pst* compared with the plants grown at 22°C after 3 DAI. Furthermore, the same study also demonstrated that *Pst* expressing the T3Es AvrRpt2 and AvrRpm1 showed 10 times more bacterial growth at 28°C compared with 22°C, indicating the plant defense responses mediated by *R*-genes are likely suppressed at higher temperatures (Wang *et al.*, 2009), and/or are affected by the virulence activity of these effectors. In support of the former, it has been demonstrated that R-protein stability is linked to the presence of SA, which, as already noted, plays an indispensable role in the plant defense response to bacterial pathogens. For example, the *R* gene-like toll/interleukin-1 receptor (TIR)-NB-LRR-type gene SUPPRESSOR OF *NPRI-1* CONSTITUTIVE1 (*SNC1*) has emerged as a case-study for SA-dependent resistance signaling and a model defining the crosstalk between the *R* genes and hormones (Zhang *et al.*, 2003; Yang & Hua, 2004). Interestingly, *SNC1* protein accumulation is reduced at elevated temperatures, a phenomenon that is coincident with the reduction of SA at elevated temperatures (Zhu *et al.*, 2010; Huot *et al.*, 2017). Using a mutagenesis-based approach, *102snc1-1* was identified, which showed pathogen resistance at both basal and elevated temperatures. This temperature-insensitive immune response in the *102snc1-1* was further attributed to the high expression level of *PRI*, further supporting the involvement of SA (Zhu *et al.*, 2010). Similarly, we observed sustained *PRI* mRNA accumulation/gene expression under elevated temperature in the *NDRI*-overexpression line.

Mounting evidence suggests that both nuclear localized TIR-NB-LRRs and plasma-membrane-localized CC-NB-LRR receptor-mediated signaling pathways in a temperature-sensitive manner (Mang *et al.*, 2012; Cheng *et al.*, 2013). Unexpectedly, in contrast to the reported suppression of *RPS2* mediated ETI

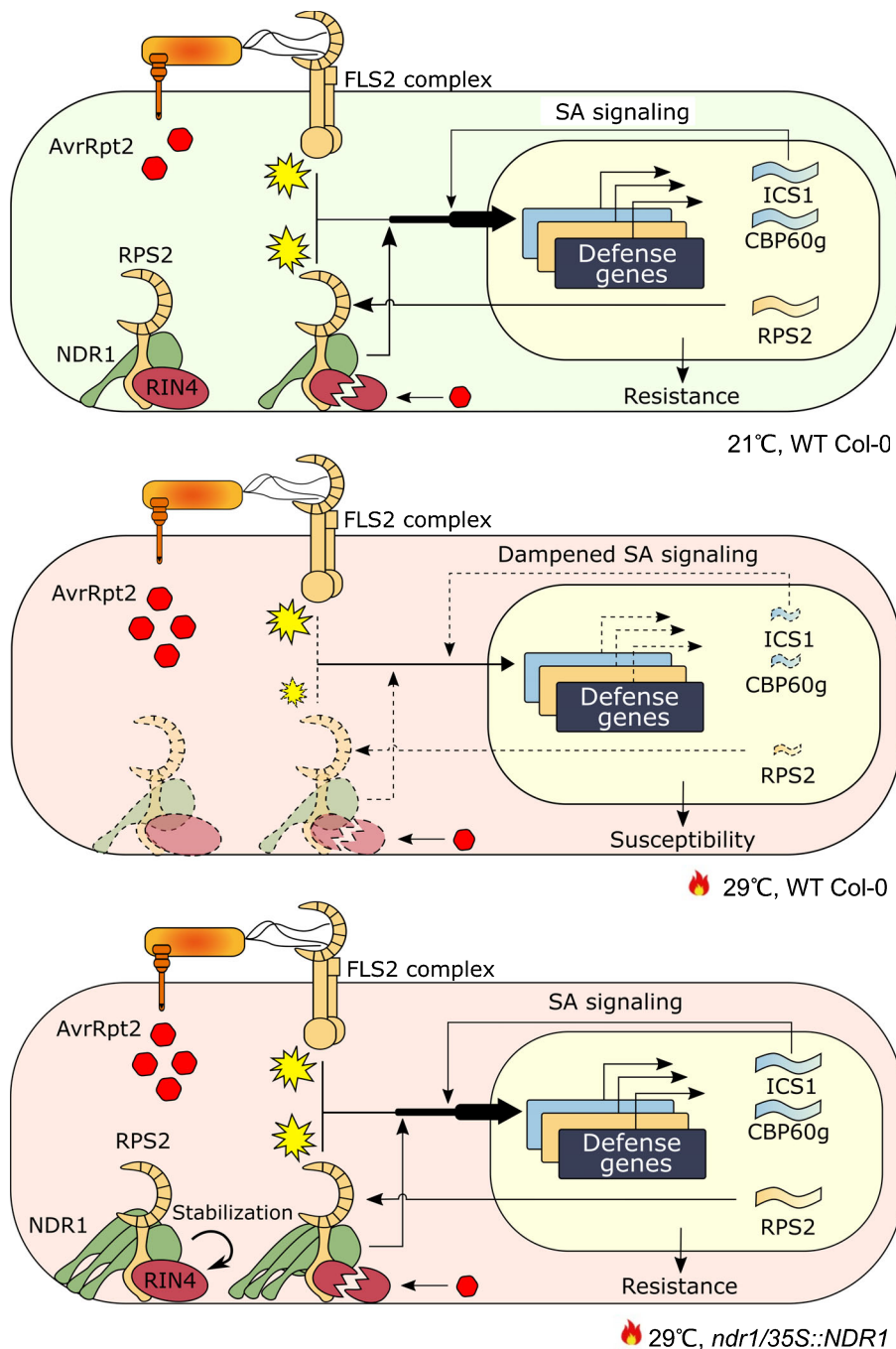


Fig. 6 The schematic diagram of the mechanism of rescued effector-triggered immunity (ETI) in elevated temperature by overexpressed *NON-RACE-SPECIFIC DISEASE RESISTANCE1* (*NDR1*) in *Arabidopsis*. In plant immunity, *NDR1* genetically interacts with Resistance to *Pseudomonas Syringae*-2 (*RPS2*) and RPM1-interacting protein 4 (*RIN4*) to facilitate ETI in response to AvrRpt2. Concomitantly, *NDR1* contributes to a robust pro-immune transcriptome, including the upregulation of *RPS2* and genes involved in salicylic acid (SA) signaling. At elevated temperature (29°C), transcription of these defense genes is inhibited, rendering plants susceptible to bacteria pathogen infection. In the *ndr1/35S::NDR1* overexpression line, increased levels of *NDR1* rescue the transcription of *ISOCHRISMATE SYNTHASE 1* (*ICS1*) and *CALMODULIN BINDING PROTEIN 60g* (*CBP60g*) under elevated temperatures, thus sustaining the production of SA and its signaling pathway. In parallel, *NDR1* overexpression enhances *RPS2* messenger RNA accumulation and stabilizes *RIN4*, the guard, to sustain the function of the nucleotide-binding leucine-rich repeat complex. Dashed lines indicate dampened signaling pathway. Yellow explosion symbols indicate immune activation.

signaling at elevated temperatures, we found that the *NDR1*-overexpression line remained resistant at elevated temperature. Previous work demonstrated that temperature acclimation at 32°C for 6 h (i.e. short-term) did not impact the mRNA accumulation of key NB-LRR signaling components (e.g. *RPM1*, *RPS2*, *RIN4*, and *NDR1*) in the absence of pathogen infection (Cheng *et al.*, 2013). Here, our data revealed the stable expression level of *RPS2* gene in the *NDR1*-overexpression line in the absence of pathogen infection under long-term (24 h) heat stress, an observation that suggests the early establishment of defense gene expression could be a preemptive strategy to defend against pathogen infection under conditions of environmental stress.

Previous results showed that *RIN4* cleavage by AvrRpt2 occurs within *c.* 8 hpi at both 23°C and 32°C (Cheng *et al.*, 2013). Consistent with this, we showed *RIN4* degradation in WT Col-0, *ndr1*, and *ics1-2* at basal and elevated temperatures. However, in the *NDR1*-overexpression line, *RIN4* remained protected from cleavage by AvrRpt2, suggesting a role of *RIN4* protection conferred by the overexpression of *NDR1*. Here, we demonstrate that BTH-induced SA production was not sufficient to protect *RIN4* from cleavage in WT Col-0, *ndr1*, and *ics1-2*, thereby eliminating the possibility of the involvement of the high levels of SA in the *NDR1*-overexpression line in the protection of *RIN4*. The simplest explanation for this is that overexpression of *NDR1*, and the

interaction of NDR1 with RIN4, protects RIN4 from cleavage. What remains unclear is how *NDR1* overexpression results in reduced effector translocation, an observation previously observed in *ics1-2* at both basal and elevated temperatures (van Dijk *et al.*, 1999; Huot *et al.*, 2017). Moreover, reduced effector translocation in the *NDR1* overexpressor would appear to be in conflict with enhanced resistance in this line (Copping *et al.*, 2004). The simplest explanation is that only a small amount of RIN4 cleavage is required for full activation of ETI, a mechanism that ensures the robust activation of resistance following release of RIN4 negative regulation. In total, we propose that the rescue of ETI in the absence of RIN4 degradation in the *NDR1*-overexpression line is potentially due to a complex interaction involving the stability of *RPS2* mRNA expression and a decrease in T3E translocation rates at elevated temperature (Fig. 6). Though much work remains towards fully defining the role of NDR1 at the nexus of biotic and abiotic signaling, the data herein provide insight into a role for NDR1 as a stabilizing component, and potential scaffolding mechanism, required for the maintenance of homeostasis during abiotic and biotic stress response signaling.









Acknowledgements

We would like to acknowledge the support of the MSU Plant Resilience Institute for providing funding to the laboratory of BD. Research in the laboratory of BD is supported by the National Institutes of General Medical Sciences (1R01GM125743) and the National Science Foundation-National Institute of Food and Agriculture (USDA) joint Plant-Biotic Interactions Program (IOS-1146128). Research in the laboratory of AM is supported by JST PRESTO (JPMJPR17Q6), Grant-in-Aid for Scientific Research (B) (19H02960), and Grant-in-Aid for Scientific Research on Innovative Areas (B) (21H05151). Research in the laboratory of KT is supported by the Fundamental Research Funds for the Central Universities (program no. 2662020ZKPY009), the Huazhong Agricultural University Scientific & Technological Self-innovation Foundation, and Joint Funding of Huazhong Agricultural University and Agricultural Genomics Institute at Shenzhen, Chinese Academy of Agricultural Sciences (SZYJY2021007). Special thanks to Alvaro Hernandez, Director of DNA Services at the Roy J. Carver Biotechnology Center, The University of Illinois, Urbana-Champaign, for providing consultation in advance of sequencing. The authors acknowledge the services of the staff at the MSU Research Technology Support Facility for conducting the LC-MS analysis, Masaki Shimono for experimental assistance, Sheng Yang He for providing the *ics1-2* seeds, and Noel Day for editorial comments. The authors declare no competing financial interests.

Author contributions

SPS and BD planned and designed the research. SPS, Y-JL and YK performed experiments. SPS, HC, Y-JL, PL, YK, AM, KT and BD analyzed data. SPS and BD wrote the paper with input from all co-authors.

ORCID

Huan Chen  <https://orcid.org/0000-0002-6584-8489>
 Brad Day  <https://orcid.org/0000-0002-9880-4319>
 Yongsig Kim  <https://orcid.org/0000-0003-3883-4951>
 Pai Li  <https://orcid.org/0000-0003-3919-3543>
 Yi-Ju Lu  <https://orcid.org/0000-0002-9590-8315>
 Akira Mine  <https://orcid.org/0000-0002-4822-4009>
 Saroopa P. Samaradivakara  <https://orcid.org/0000-0002-8637-8738>
 Kenichi Tsuda  <https://orcid.org/0000-0001-7074-0731>

Data availability

The RNA-seq data generated herein are contained within the National Center for Biotechnology Information Short Read Archive. The Illumina RNA-seq reads were deposited in BioProject under project ID PRJNA778239.

References

- Anders S, Pyl PT, Huber W. 2015. HTSEQ – a PYTHON framework to work with high-throughput sequencing data. *Bioinform* 31: 166–169.
- Axtell MJ, Chisholm ST, Dahlbeck D, Staskawicz BJ. 2003. Genetic and molecular evidence that the *Pseudomonas syringae* type III effector protein AvrRpt2 is a cysteine protease. *Molecular Microbiology* 49: 1537–1546.
- Axtell MJ, Staskawicz BJ. 2003. Initiation of *RPS2*-specified disease resistance in *Arabidopsis* is coupled to the AvrRpt2-directed elimination of RIN4. *Cell* 112: 369–377.
- Bahuguna RN, Jagadish KSV. 2015. Temperature regulation of plant phenological development. *Environmental and Experimental Botany* 111: 83–90.
- Balasubramanian S, Sureshkumar S, Lempe J, Weigel D. 2006. Potent induction of *Arabidopsis thaliana* flowering by elevated growth temperature. *PLoS Genetics* 2: e106.
- Bao Y, Song W-M, Pan J, Jiang C-M, Srivastava R, Li B, Zhu L-Y, Su H-Y, Gao X-S, Liu H *et al.* 2016. Overexpression of the *NDR1/HIN1*-Like Gene *NHL6* modifies seed germination in response to abscisic acid and abiotic stresses in *Arabidopsis*. *PLoS ONE* 11: e0148572.
- Berens ML, Wolinska KW, Spaepen S, Ziegler J, Nobori T, Nair A, Kruler V, Winkelmuller TM, Wang Y, Mine A *et al.* 2019. Balancing trade-offs between biotic and abiotic stress responses through leaf age-dependent variation in stress hormone cross-talk. *Proceedings of the National Academy of Sciences, USA* 116: 2364–2373.
- Bolger AM, Lohse M, Usadel B. 2014. TRIMMOMATIC: a flexible trimmer for Illumina sequence data. *Bioinformatics* 30: 2114–2120.
- Catinot J, Buchala A, Abou-Mansour E, Métraux JP. 2008. Salicylic acid production in response to biotic and abiotic stress depends on isochorismate in *Nicotiana benthamiana*. *FEBS Letters* 582: 473–478.
- Century KS, Holub EB, Staskawicz BJ. 1995. NDR1, a locus of *Arabidopsis thaliana* that is required for disease resistance to both a bacterial and a fungal pathogen. *Proceedings of the National Academy of Sciences, USA* 92: 6597–6601.
- Century KS, Shapiro AD, Repetti PP, Dahlbeck D, Holub E, Staskawicz BJ. 1997. NDR1, a pathogen-induced component required for *Arabidopsis* disease resistance. *Science* 278: 1963–1965.
- Chakravarthy S, Huot B, Kvitko BH. 2017. Effector translocation: Cya reporter assay. In: L. Journet and E. Cascales, eds. *Bacterial protein secretion systems: methods and protocols*. New York, NY, USA: Springer, 473–487.
- Cheng C, Gao X, Feng B, Sheen J, Shan L, He P. 2013. Plant immune response to pathogens differs with changing temperatures. *Nature Communications* 4: 2530.
- Chisholm ST, Dahlbeck D, Krishnamurthy N, Day B, Sjolander K, Staskawicz BJ. 2005. Molecular characterization of proteolytic cleavage sites of the *Pseudomonas syringae* effector AvrRpt2. *Proceedings of the National Academy of Sciences, USA* 102: 2087–2092.

- Coppinger P, Repetti PP, Day B, Dahlbeck D, Mehlert A, Staskawicz BJ. 2004. Overexpression of the plasma membrane-localized NDR1 protein results in enhanced bacterial disease resistance in *Arabidopsis thaliana*. *The Plant Journal* 40: 225–237.
- Day B, Dahlbeck D, Staskawicz BJ. 2006. NDR1 interaction with RIN4 mediates the differential activation of multiple disease resistance pathways in *Arabidopsis*. *Plant Cell* 18: 2782–2791.
- De Vleeschauwer D, Xu J, Hofte M. 2014. Making sense of hormone-mediated defense networking: from rice to *Arabidopsis*. *Frontiers in Plant Science* 5: 611.
- van Dijk K, Fouts DE, Rehm AH, Hill AR, Collmer A, Alfano JR. 1999. The Avr (effector) proteins HrmA (HopPsyA) and AvrPto are secreted in culture from *Pseudomonas syringae* pathovars via the Hrp (type III) protein secretion system in a temperature- and pH-sensitive manner. *Journal of Bacteriology* 181: 4790–4797.
- Du Z, Zhou X, Ling Y, Zhang Z, Su Z. 2010. AGRIGO: a GO analysis toolkit for the agricultural community. *Nucleic Acids Research* 38: W64–W70.
- Eisen MB, Spellman PT, Brown PO, Botstein D. 1998. Cluster analysis and display of genome-wide expression patterns. *Proceedings of the National Academy of Sciences, USA* 95: 14863–14868.
- Elmore JM, Lin ZJ, Coaker G. 2011. Plant NB-LRR signaling: upstreams and downstreams. *Current Opinion in Plant Biology* 14: 365–371.
- Fu ZQ, Guo M, Alfano JR. 2006. *Pseudomonas syringae* HrpJ is a type III secreted protein that is required for plant pathogenesis, injection of effectors, and secretion of the HrpZ1 harpin. *Journal of Bacteriology* 188: 6060–6069.
- Gimenez E, Salinas M, Manzano-Agugliaro F. 2018. Worldwide research on plant defense against biotic stresses as improvement for sustainable agriculture. *Sustainability* 10: 391.
- Guo Q, Major IT, Howe GA. 2018. Resolution of growth-defense conflict: mechanistic insights from jasmonate signaling. *Current Opinion in Plant Biology* 44: 72–81.
- Guo Z, Wang X, Hu Z, Wu C, Shen Z. 2021. The pentatricopeptide repeat protein GEND1 is required for root development and high temperature tolerance in *Arabidopsis thaliana*. *Biochemical and Biophysical Research Communications* 578: 63–69.
- Havko NE, Kapali G, Das MR, Howe GA. 2020. Stimulation of insect herbivory by elevated temperature outweighs protection by the jasmonate pathway. *Plants* 9: 172.
- Hossain MA, Li ZG, Hoque TS, Burritt DJ, Fujita M, Munne-Bosch S. 2018. Heat or cold priming-induced cross-tolerance to abiotic stresses in plants: key regulators and possible mechanisms. *Protoplasma* 255: 399–412.
- Hu Y, Dong Q, Yu D. 2012. *Arabidopsis* WRKY46 coordinates with WRKY70 and WRKY53 in basal resistance against pathogen *Pseudomonas syringae*. *Plant Science* 185–186: 288–297.
- Huot B, Castroverde CDM, Velasquez AC, Hubbard E, Pulman JA, Yao J, Childs KL, Tsuda K, Montgomery BL, He SY. 2017. Dual impact of elevated temperature on plant defence and bacterial virulence in *Arabidopsis*. *Nature Communications* 8: 1808.
- Iqbal Z, Iqbal MS, Hashem A, Abd Allah EF, Ansari MI. 2021. Plant defense responses to biotic stress and its interplay with fluctuating dark/light conditions. *Frontiers in Plant Science* 12: 631810.
- Jones JD, Dangl JL. 2006. The plant immune system. *Nature* 444: 323–329.
- Kim D, Langmead B, Salzberg SL. 2015. HISAT: a fast spliced aligner with low memory requirements. *Nature Methods* 12: 357–360.
- Kim HS, Desveaux D, Singer AU, Patel P, Sondel J, Dangl JL. 2005. The *Pseudomonas syringae* effector AvrRpt2 cleaves its c-terminally acylated target, RIN4, from *Arabidopsis* membranes to block RPM1 activation. *Proceedings of the National Academy of Sciences, USA* 102: 6496–6501.
- Kim Y, Gilmour SJ, Chao L, Park S, Thomashow MF. 2020. *Arabidopsis* CAMTA transcription factors regulate piperolic acid biosynthesis and priming of immunity genes. *Molecular Plant* 13: 157–168.
- Knepper C, Savory EA, Day B. 2011. *Arabidopsis* NDR1 is an integrin-like protein with a role in fluid loss and plasma membrane-cell wall adhesion. *Plant Physiology* 156: 286–300.
- Koini MA, Alvey L, Allen T, Tilley CA, Harberd NP, Whitlam GC, Franklin KA. 2009. High temperature-mediated adaptations in plant architecture require the bHLH transcription factor PIF4. *Current Biology* 19: 408–413.
- Kouzai Y, Noutoshi Y, Inoue K, Shimizu M, Onda Y, Mochida K. 2018. Benzothiadiazole, a plant defense inducer, negatively regulates sheath blight resistance in *Brachypodium distachyon*. *Scientific Reports* 8: 17358.
- Kunkel BN, Bent AF, Dahlbeck D, Innes RW, Staskawicz BJ. 1993. RPS2, an *Arabidopsis* disease resistance locus specifying recognition of *Pseudomonas syringae* strains expressing the avirulence gene *avrRpt2*. *Plant Cell* 5: 865–875.
- Langfelder P, Horvath S. 2008. WGCNA: an R package for weighted correlation network analysis. *BMC Bioinformatics* 9: 559.
- Lee HJ, Jung JH, Cortes Llorca L, Kim SG, Lee S, Baldwin IT, Park CM. 2014. FCA mediates thermal adaptation of stem growth by attenuating auxin action in *Arabidopsis*. *Nature Communications* 5: 5473.
- Li L, Li RF, Ming ZH, Lu GT, Tang JL. 2017. Identification of a novel type III secretion-associated outer membrane-bound protein from *Xanthomonas campestris* pv. *campestris*. *Scientific Reports* 7: 42724.
- Li L-S, Ying J, Li E, Ma T, Li M, Gong L-M, Wei G, Zhang Y, Li S. 2021. *Arabidopsis* CBP60b is a central transcriptional activator of immunity. *Plant Physiology* 186: 1645–1659.
- Li P, Day B. 2019. Battlefield cytoskeleton: turning the tide on plant immunity. *Molecular Plant–Microbe Interactions* 32: 25–34.
- Li P, Lu Y-J, Chen H, Day B. 2020. Lifecycle of the plant immune response. *Critical Reviews in Plant Sciences* 39: 72–100.
- Li S, Zhou X, Chen L, Huang W, Yu D. 2010. Functional characterization of *Arabidopsis thaliana* WRKY39 in heat stress. *Molecules and Cells* 29: 475–483.
- Li Z, Liu H, Ding Z, Yan J, Yu H, Pan R, Hu J, Guan Y, Hua J. 2020. Low temperature enhances plant immunity via salicylic acid pathway genes that are repressed by ethylene. *Plant Physiology* 182: 626–639.
- Liu L, Sonbol FM, Huot B, Gu Y, Withers J, Mwimba M, Yao J, He SY, Dong X. 2016. Salicylic acid receptors activate jasmonic acid signalling through a non-canonical pathway to promote effector-triggered immunity. *Nature Communications* 7: 13099.
- Lu H. 2009. Dissection of salicylic acid-mediated defense signaling networks. *Plant Signaling & Behavior* 4: 713–717.
- Lu H, Zhang C, Albrecht U, Shimizu R, Wang G, Bowman KD. 2013. Overexpression of a citrus NDR1 ortholog increases disease resistance in *Arabidopsis*. *Frontiers in Plant Science* 4: 157.
- Lu Y-J, Chen H, Corrier A, Buyuk I, Li P, Samaradivakara S, Wai CM, Sakamoto H, Santos P, VanBuren R *et al.* 2021. NDR1 and the *Arabidopsis* plasma membrane ATPase AHA5 are required for processes that converge on drought tolerance and immunity. *bioRxiv*. doi: 10.1101/2021.06.10.445978.
- Mackey D, Belkhadir Y, Alonso JM, Ecker JR, Dangl JL. 2003. *Arabidopsis* RIN4 is a target of the type III virulence effector AvrRpt2 and modulates RPS2-mediated resistance. *Cell* 112: 379–389.
- Maier BA, Kiefer P, Field CM, Hemmerle L, Bortfeld-Miller M, Emmenegger B, Schafer M, Pfeilmeier S, Sunagawa S, Vogel CM *et al.* 2021. A general non-self response as part of plant immunity. *Nature Plants* 7: 696–705.
- Mang HG, Qian W, Zhu Y, Qian J, Kang HG, Klessig DF, Hua J. 2012. Abscisic acid deficiency antagonizes high-temperature inhibition of disease resistance through enhancing nuclear accumulation of resistance proteins SNC1 and RPS4 in *Arabidopsis*. *Plant Cell* 24: 1271–1284.
- McClung CR, Davis SJ. 2010. Ambient thermometers in plants: from physiological outputs towards mechanisms of thermal sensing. *Current Biology* 20: R1086–R1092.
- Miller RN, Costa Alves GS, Van Sluys MA. 2017. Plant immunity: unravelling the complexity of plant responses to biotic stresses. *Annals of Botany* 119: 681–687.
- Mine A, Seyfferth C, Kracher B, Berens ML, Becker D, Tsuda K. 2018. The defense phytohormone signaling network enables rapid, high-amplitude transcriptional reprogramming during effector-triggered immunity. *Plant Cell* 30: 1199–1219.
- Mudgett MB. 2005. New insights to the function of phytopathogenic bacterial type III effectors in plants. *Annual Review of Plant Biology* 56: 509–531.
- Nejat N, Mantri N. 2017. Plant immune system: crosstalk between responses to biotic and abiotic stresses the missing link in understanding plant defence. *Current Issues in Molecular Biology* 23: 1–16.
- Penfield S. 2008. Temperature perception and signal transduction in plants. *New Phytologist* 179: 615–628.

- Quint M, Delker C, Franklin KA, Wigge PA, Halliday KJ, van Zanten M. 2016. Molecular and genetic control of plant thermomorphogenesis. *Nature Plants* 2: 15190.
- Saijo Y, Loo EP. 2020. Plant immunity in signal integration between biotic and abiotic stress responses. *New Phytologist* 225: 87–104.
- Sakata T, Oshino T, Miura S, Tomabechi M, Tsunaga Y, Higashitani N, Miyazawa Y, Takahashi H, Watanabe M, Higashitani A. 2010. Auxins reverse plant male sterility caused by high temperatures. *Proceedings of the National Academy of Sciences, USA* 107: 8569–8574.
- Samuel G. 1931. Some experiments on inoculating methods with plant viruses, and on local lesions. *The Annals of Applied Biology* 18: 494–507.
- Shannon P, Markiel A, Ozier O, Baliga NS, Wang JT, Ramage D, Amin N, Schwikowski B, Ideker T. 2003. CYTOSCAPE: a software environment for integrated models of biomolecular interaction networks. *Genome Research* 13: 2498–2504.
- Strawn MA, Marr SK, Inoue K, Inada N, Zubieta C, Wildermuth MC. 2007. *Arabidopsis* isochorismate synthase functional in pathogen-induced salicylate biosynthesis exhibits properties consistent with a role in diverse stress responses. *Journal of Biological Chemistry* 282: 5919–5933.
- Tao Y, Xie Z, Chen W, Glazebrook J, Chang H-S, Han B, Zhu T, Zou G, Katagiri F. 2003. Quantitative nature of *Arabidopsis* responses during compatible and incompatible interactions with the bacterial pathogen *Pseudomonas syringae*. *Plant Cell* 15: 317–330.
- Tsuda K, Sato M, Stoddard T, Glazebrook J, Katagiri F. 2009. Network properties of robust immunity in plants. *PLoS Genetics* 5: e1000772.
- Tsuda K, Somssich IE. 2015. Transcriptional networks in plant immunity. *New Phytologist* 206: 932–947.
- Velasquez AC, Oney M, Huot B, Xu S, He SY. 2017. Diverse mechanisms of resistance to *Pseudomonas syringae* in a thousand natural accessions of *Arabidopsis thaliana*. *New Phytologist* 214: 1673–1687.
- Venkatesh J, Kang BC. 2019. Current views on temperature-modulated R gene-mediated plant defense responses and tradeoffs between plant growth and immunity. *Current Opinion in Plant Biology* 50: 9–17.
- Wang Y, Bao Z, Zhu Y, Hua J. 2009. Analysis of temperature modulation of plant defense against biotrophic microbes. *Molecular Plant–Microbe Interactions* 22: 498–506.
- Wang Y, Hua J. 2009. A moderate decrease in temperature induces COR15a expression through the CBF signaling cascade and enhances freezing tolerance. *The Plant Journal* 60: 340–349.
- van Wersch S, Tian L, Hoy R, Li X. 2020. Plant NLRs: the whistleblowers of plant immunity. *Plant Communications* 1: 100016.
- Yang S, Hua J. 2004. A haplotype-specific resistance gene regulated by *BONZAI1* mediates temperature-dependent growth control in *Arabidopsis*. *Plant Cell* 16: 1060–1071.
- Yuan M, Ngou BPM, Ding P, Xin XF. 2021. PTI-ETI crosstalk: an integrative view of plant immunity. *Current Opinion in Plant Biology* 62: 102030.
- Zhang H, Zhu J, Gong Z, Zhu JK. 2022. Abiotic stress responses in plants. *Nature Reviews Genetics* 23: 104–119.
- Zhang Y, Goritschnig S, Dong X, Li X. 2003. A gain-of-function mutation in a plant disease resistance gene leads to constitutive activation of downstream signal transduction pathways in suppressor of *npr1-1*, constitutive 1. *Plant Cell* 15: 2636–2646.
- Zhao J, Lu Z, Wang L, Jin B. 2020. Plant responses to heat stress: physiology, transcription, noncoding RNAs, and epigenetics. *International Journal of Molecular Sciences* 22: 117.
- Zhu Y, Qian W, Hua J. 2010. Temperature modulates plant defense responses through NB-LRR proteins. *PLoS Pathogens* 6: e1000844.

Supporting Information

Additional Supporting Information may be found online in the Supporting Information section at the end of the article.

Fig. S1 Temporal dynamics of transcriptome responses to heat stress.

Fig. S2 Venn diagrams illustrating the overlap between *NDRI*-dependent genes and heat-responsive genes.

Fig. S3 mRNA accumulation of key defense response genes.

Fig. S4 Expression patterns of coexpression modules.

Fig. S5 Disease assays at 0 hpi after avirulent phytopathogen bacteria treatment.

Fig. S6 Temporal detection of RIN4 after virulent *Pst* treatment.

Fig. S7 Hypersensitive response and disease phenotypes after treatment with *Pst-AvrRpm1* and *Pst-AvrPphB*.

Fig. S8 Disease assays at 3 dpi after avirulent phytopathogen bacteria treatment.

Fig. S9 Bacterial growth after syringe-infiltration with *Pst*-expressing *hrcC* and *AvRpt2-CyaA* in wild-type (Col-0) and mutant plants.

Fig. S10 Benzothiadiazole (BTH)-induced SA does not protect RIN4 under *Pst-AvrRpt2* treatment.

Fig. S11 Bacterial growth at 0 hpi in BTH-untreated wild-type (Col-0) and mutant plants after syringe-infiltration with mock and *Pst*-expressing *AvrRpt2-Cya*.

Table S1 Mean centered expression levels (\log_2) of differentially expressed genes.

Table S2 Differentially expressed genes in cluster 1.

Table S3 Gene ontology enrichment of cluster 1 containing genotype-independent temperature-responsive genes (FDR < 0.05).

Table S4 Differentially expressed genes in cluster 2.

Table S5 Gene Ontology enrichment of cluster 2 containing genotype-specific temperature-responsive genes (FDR < 0.05).

Table S6 The number of upregulated genes between genotypes.

Table S7 The number of downregulated genes between genotypes.

Table S8 *NDRI*-upregulated genes, heat-suppressed genes, and their intersections at 6 h.

Table S9 *NDRI*-downregulated genes, heat-induced genes, and their intersections at 6 h.

Table S10 *NDRI*-upregulated genes, heat-suppressed genes, and their intersections at 24 h.

Table S11 *NDR1*-downregulated genes, heat-induced genes, and their intersections at 24 h.

Table S12 Gene Ontology enrichment of *NDR1*-upregulated genes, heat-suppressed genes at 6 h.

Table S13 Gene Ontology enrichment of *NDR1*-downregulated genes, heat-induced genes at 6 h.

Table S14 Gene Ontology enrichment of *NDR1*-upregulated genes, heat-suppressed genes at 24 h.

Table S15 Gene Ontology enrichment of *NDR1*-downregulated genes, heat-induced genes at 24 h.

Table S16 Gene Ontology enrichment analysis of the genes in each coexpression module (FDR < 0.05).

Table S17 Description of the genes in each coexpression module.

Table S18 Quantification of RIN4 after virulent *Pst* treatment.

Please note: Wiley Blackwell are not responsible for the content or functionality of any Supporting Information supplied by the authors. Any queries (other than missing material) should be directed to the *New Phytologist* Central Office.